Quaternion-valued short term forecasting of wind profile

C. Cheong Took, D. P. Mandic and K. Aihara

***Abstract*— This work presents novel methodology for the simultaneous modelling and forecasting of three-dimensional (3D) wind fields. This is achieved based on a quaternion domain wind model, which naturally accounts for the coupling between the dimensions of the 3D wind field. The proposed quaternion valued processing also facilitates the fusion of external atmospheric parameters, such as air temperature, exhibiting more degrees of freedom and enhanced accuracy. The quaternion least mean square (QLMS) algorithm and its variants are used for short term adaptive forecasting, and a rigorous comparative study with the corresponding algorithms in $\mathbb{R}^4$ is performed. Simulations for different wind regimes and over a range of prediction horizons support the approach.**

I. Introduction

Wind farm technology is becoming increasingly important, and governments of many countries are committed to introducing the so-called "green" energy sources [1]. However, the intermittent nature of wind and a conservative manner in which wind farms (WFs) currently operate, hinder the practical efficiency of wind turbines (WTs). For instance, WTs have to be switched off during strong winds, and at milder winds it is not always cost effective to integrate WTs into the grid. In addition, Betz's momentum theory states that only less than 60% of the wind power can be converted to mechanical power given ideal airflow and lossless conversion [2]. To increase the efficiency of WTs, vector controls can be employed to give faster response which, in turn, results in improved stability and enhanced output performance [1].

Recently, the modelling of wind has been recognised as a crucial component in control technology within WFs [3], especially in short-term wind forecasting [4]- [7]. One convenient way to represent wind field is to consider simultaneously wind speed and direction as a complex-valued quantity [7]- [8] as illustrated in Fig. 1. This way, we account naturally for the statistical dependence between the speed and direction and avoid the undermodelling errors introduced by standard dual univariate models [9]. In the complex domain, the wind vector $\mathbf{v}(k)$ can be expressed as

$$\mathbf{v}(n) = |\mathbf{v}(n)| \exp^{\imath\theta(n)} = v_E(n) + \imath v_N(n) \qquad (1)$$

where θ, $|\mathbf{v}(n)|$, $v_E(n)$, and $v_N(n)$ denote respectively the direction, magnitude, wind speed in the east-west direction, and wind speed in the north-south direction, and $\imath = \sqrt{-1}$. In doing so, we can exploit the time-varying correlation between each dimension of the signal, and thereby improve the accuracy.

C. Cheong Took and D. P. Mandic are with the Department of Electrical and Electronic Engineering, Imperial College London, London SW7 2AZ, United Kingdom; emails: {c.cheong-took, d.mandic}@ic.ac.uk

K. Aihara is with the Institute of Industrial Science, University of Tokyo, Tokyo, Japan; email: aihara@sat.t.u-tokyo.ac.jp

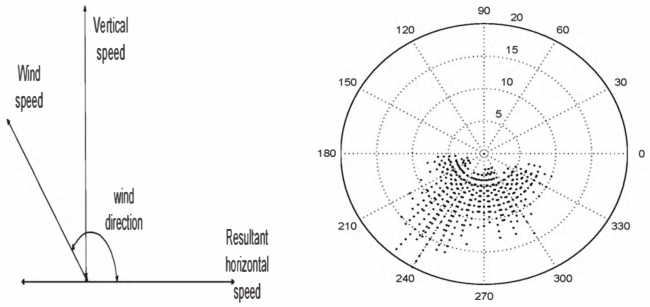

Fig. 1. Wind data model and the amplitude distribution: *Left*: a complex-valued representation, *Right*: wind lattice.

This model is supported by physical evidence, as both wind speed and direction influence the power output P generated by the WT [2], according to

$$P = \frac{1}{2}\rho C A \omega^3 \qquad (2)$$

where ρ denotes the air density, A the area swept by the rotor, ω the wind velocity and C the power coefficient. In particular, the power coefficient C depends on the blade pitch angle (design parameter) that ensures an optimal angle of attack (aerodynamic parameter) between the chord of the blade and the incoming free-stream wind [2]. Hence, the direction of the wind θ affects the power coefficient, although in most present studies this is not taken into account. Wind direction is of crucial importance, when it comes to spatial correlation studies, concerned with the position of the WT in a wind park [10]. The complex domain modelling also allows for the use of new developments in complex statistics - so called augmented statistics, to account for the noncircular distributions and nonstationarity of the intermittent wind signals. More details can be found in [8], [12]–[14].

Temperature T is another factor that influences the power model of WTs. By expressing the air density as [11]

$$\rho = \frac{353.049}{T} e^{-0.034\frac{E}{T}} \qquad (3)$$

where E denotes the elevation, and by substituting (3) into (2), the output power of a WT

$$P = \frac{176.525}{T} C A \omega^3 e^{-0.034\frac{E}{T}} \qquad (4)$$

is clearly a function of air temperature. This particularly affects offshore WTs, as nocturnal and diurnal temperatures can differ by an order of magnitude.

978-1-4244-8126-2/10/$26.00 ©2010 IEEE

Although the recently introduced complex-valued model [7], and its statistically more efficient version [8] outperformed standard models, they can operate only in the horizontal plane. On the other hand, wind is a three-dimensional phenomenon, and the modelling of its behaviour (turbulence, gusts) would benefit from the use of appropriate 3D models. The aim of this work is therefore to develop a new framework for direct three-dimensional short term wind forecasting.

This is achieved based on adaptive prediction in the quaternion domain $\mathbb{H}$, where the 3D wind field is represented by a pure quaternion $\mathbf{q}(n)$ as shown in Fig. 2. In addition, following the recently introduced "data

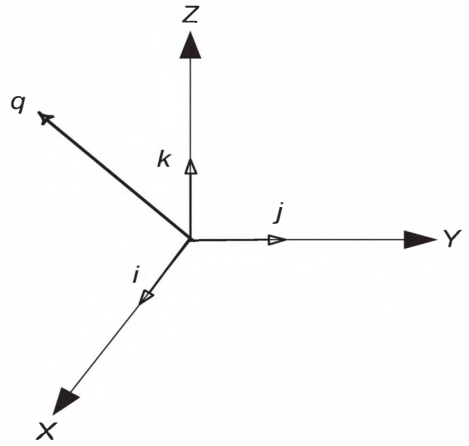

Fig. 2. A three-dimensional wind vector as a pure quaternion q.

fusion via vector spaces" framework [12]- [13] an external parameter, e.g. air temperature can be incorporated as the fourth dimension of a full quaternion to enhance the performance.

Theoretical background of this problem has been introduced in [15]. In this work, a comprehensive study of real-time wind forecasting for various wind regimes is performed, at various degrees of averaging, and for varying prediction horizons. The proposed forecasting model is based on the recently introduced quaternion LMS (QLMS) [15], [16] and the results are compared against those obtained by its real domain counterpart – the multi-channel LMS (MLMS) [17].

II. Wind characteristics and forecasting framework

In our recent work, we studied direct multidimensional wind models, their local predictability and correlation between wind signal components [7]- [8]. These studies suggested that the wind signal variables (speed, direction) should be considered as one entity, e.g. a complex-valued quantity rather than two univariate real variables. We here extend this work by treating wind measurements as hypercomplex quaternion-valued compact signals.

A. The forecasting framework in $\mathbb{R}^4$

Adaptive prediction can be performed either in a direct or recursive manner [18]. We use the recursive approach as it is better equipped to deal with the bias in estimation. Based on the history of the data (delay vector) the predictor estimates the signal value at M steps ahead of the current time instant k, by using previously estimated values at $n-1, \ldots, n-L+1$. A standard way to perform the modelling of four-dimensional (4D) data is via multichannel models in $\mathbb{R}^4$. For the 3D and 4D wind modelling we consider the real valued multi-channel LMS (MLMS) [17], where the qth output of the adaptive filter is given by

$$y_q(n) = \sum_{p=1}^{4} \mathbf{h}_{pq}^T(n)\mathbf{x}_p(n) \qquad q = 1, \ldots, 4 \tag{5}$$

where the pth input data vector is denoted by $\mathbf{x}_p(n) = [x_p(n), \ldots, x_p(n-L+1)]^T$, the adaptive filter coefficients are $\mathbf{h}_{pq}(n) = [h_{pq}(n), \ldots, h_{pq}(n-L+1)]^T$, L is tap input length and $(\cdot)^T$ the vector transpose operator. The error signal $e_q(n)$ used for the adaptation of the adaptive filter weights can be expressed as

$$e_q(n) = d_q(n) - y_q(n) \tag{6}$$

The adaptation of the pqth filter coefficient vector is performed using the steepest descent approach, that is

$$\mathbf{h}_{pq}(n+1) = \mathbf{h}_{pq}(n) - \mu \nabla_{\mathbf{h}_{pq}} \mathcal{J}_q(n)_{|_{\mathbf{h}_{pq}=\mathbf{h}_{pq}(n)}} \tag{7}$$

where μ is the rate of adaptation (stepsize) and $\mathcal{J}_q(n)$ is the cost function defined as the total error power

$$\mathcal{J}(n) = \sum_{q=1}^{4} e_q^2(n) \tag{8}$$

Based on (7)-(8), every weight vector $\mathbf{h}_{pq}$ of the four-channel LMS algorithm is given by [17]

$$\mathbf{h}_{pq}(n+1) = \mathbf{h}_{pq}(n) - \mu e_q(n)\mathbf{x}_p(n) \qquad p, q = 1, \ldots, 4 \tag{9}$$

Notice that the correlation between the channels is taken into account by the product of error $e_q(n)$ and the tap delay vector $\mathbf{x}_p(n)$.

III. Quaternion-valued adaptive prediction

Quaternions were conceived by W. Hamilton in 1843 as a hypercomplex extension to complex numbers. To date, quaternions have found various applications in signal processing such as in digital filters [19] [20], texture segmentation [21], spectrum analysis [22] and singular value decomposition algorithms for vector sensing [23]. A quaternion variable u comprises of a real/scalar part $\Re\{u\}$, denoted with the subscript a, and a vector part $\Im\{u\}$ consisting of three

imaginary parts (denoted by subscripts b, c, d), and can be expressed as

$$\begin{aligned} u &= [\Re\{u\}, \Im\{u\}] = [u_a, \mathbf{u}] \quad \in \mathbb{H} \\ &= [u_a, (u_b, u_c, u_d)] \\ &= u_a + u_b\imath + u_c\jmath + u_d\kappa \quad \{u_a, u_b, u_c, u_d \in \mathbb{R}\} \end{aligned} \tag{10}$$

where the relationships between the imaginary parts are

$$\begin{aligned} \imath\jmath &= \kappa \qquad \jmath\imath = -\kappa \\ \jmath\kappa &= \imath \qquad \kappa\jmath = -\imath \\ \kappa\imath &= \jmath \qquad \imath\kappa = -\jmath \end{aligned}$$

$$\imath\jmath\kappa = \imath^2 = \jmath^2 = \kappa^2 = -1 \tag{11}$$

Notice that the non-commutativity of the quaternion product is implicitly implied in the first three lines of (11). The quaternion product can be calculated as

$$u_1 u_2 = [u_{a,1}, \mathbf{u}_1][u_{a,2}, \mathbf{u}_2]$$

$$u_1 u_2 = [u_{a,1}u_{a,2} - \mathbf{u}_1 \cdot \mathbf{u}_2,\ u_{a,1}\mathbf{u}_2 + u_{a,2}\mathbf{u}_1 + \mathbf{u}_1 \times \mathbf{u}_2] \tag{12}$$

where $u = u_a + u_b\imath + u_c\imath + u_d\kappa = [u_a, \mathbf{u}]$, and symbols "$\cdot$" and "$\times$" denote respectively the dot-product and the outer-product. Other important operations in quaternion algebra are the quaternion conjugate $u^* = [u_a, \mathbf{u}]^* = [u_a, -\mathbf{u}]$, and the quaternion norm $||u||_2^2 = uu^*$. The anti-involution property of the quaternion conjugation can be expressed as $(u_1 u_2)^* = u_2^* u_1^*$. A quaternion variable is said to be pure, when its real part vanishes.

A. Derivation of the Quaternion Least Mean Square (QLMS) Algorithm

Based on the properties of quaternion algebra, we shall now introduce the QLMS algorithm for finite impulse response (FIR) adaptive filters. The cost function $\mathcal{J}(n)$ is the instantaneous squared error (error power) given by

$$\begin{aligned} \mathcal{J}(n) &= e(n)e^*(n) \\ &= e_a^2(n) + e_b^2(n) + e_c^2(n) + e_d^2(n) \\ &= d(n)d^*(n) + y(n)y^*(n) - y(n)d^*(n) \\ &\quad -d(n)y^*(n) \end{aligned} \tag{13}$$

where the error $e(n) = d(n) - \mathbf{w}^T(n)\mathbf{x}(n)$ is quaternion valued, with $d(n)$, $\mathbf{w}(n)$, and $\mathbf{x}(n)$ denoting respectively the teaching signal, adaptive weight vector, and filter input. Notice that the cost function (13) is real-valued, as it represents a product of a quaternion-valued variable and its conjugate. The adaptive predictor output $y(n)$ is given by

$$y(n) = \mathbf{w}^T(n)\mathbf{x}(n) = \sum_{m=1}^{L} w_m(n)x(n-m) \tag{14}$$

To update the mth adaptive filter coefficient $w_m(n)$, we need to calculate the following gradient

$$\begin{aligned} \nabla_{w_m}\big(\mathcal{J}(n)\big) &= \nabla_{w_m}\big(y(n)y^*(n)\big) - \nabla_{w_m}\big(y(n)d^*(n)\big) \\ &\quad -\nabla_{w_m}\big(d(n)y^*(n)\big) \end{aligned} \tag{15}$$

where

$$\begin{aligned} \nabla_{w_m}\big(y(n)y^*(n)\big) &= 4y(n)x^*(n-m) \\ &\quad -2x^*(n-m)y^*(n) \\ \nabla_{w_m}\big(y(n)d^*(n)\big) &= -2x^*(n-m)d^*(n) \\ \nabla_{w_m}\big(d(n)y^*(n)\big) &= 4d(n)x^*(n-m) \end{aligned}$$

Using the rules of quaternion algebra, this gives

$$\begin{aligned} \nabla_{w_m}\big(\mathcal{J}(n)\big) &= 4y(n)x^*(n-m) - 2x^*(n-m)y^*(n) \\ &\quad +2x^*(n-m)d^*(n) - 4d(n)x^*(n-m) \\ &= 4\big(y(n) - d(n)\big)x^*(n-m) \\ &\quad -2x^*(n-m)\big(y^*(n) - d^*(n)\big) \\ &= -2\big(2e(n)x^*(n-m) \\ &\quad -x^*(n-m)e^*(n)\big) \end{aligned} \tag{16}$$

Finally, the update of the mth adaptive weight coefficient of QLMS can be expressed as [15]

$$\begin{aligned} w_m(n+1) &= w_m(n) - \mu\nabla_{w_m}\big(\mathcal{J}(n)\big) \\ &= w_m(n) + \mu\Big(2e(n)x^*(n-m) - x^*(n-m)e^*(n)\Big) \end{aligned} \tag{17}$$

where the factor 2 in (16) can be absorbed by the stepsize μ. This concludes the the derivation of the quaternion LMS (QLMS) algorithm, for more detail see [15].

IV. Simulation results

To demonstrate the benefits of the direct multidimensional approach, two sets of experiments were conducted. The first dataset was recorded in a controlled/closed environment at Imperial College London (ICL). The second dataset was recorded in an open urban environment at the Institute of Industrial Science (IIS) at the University of Tokyo. Factors that may affect the statistics of wind signal are the sampling frequency (F_s), the degree of averaging (downsampling), and the environment considered (that is, closed or open space) [8]. Table I illustrates statistical properties of the two sets of wind data recorded in different conditions at ICL and IIS. Both data sets were four-dimensional and comprised wind

TABLE I

Statistical properties of the wind data sets. 'Avg', 'Max', 'Min' and 'Std' denote the mean, maximum, minimum and standard deviation velocity.

	Controlled environment (F_s = 32 Hz)			*Open space* (F_s = 50 Hz)		
	x-axis	y-axis	z-axis	x-axis	y-axis	z-axis
Samples	2000	2000	2000	45,000	45,000	45,000
Avg (m/s)	-0.06	-0.38	-0.11	-0.08	-0.45	-0.02
Max (m/s)	1.93	3.42	1.13	0.99	1.55	1.27
Min (m/s)	-1.72	-2.89	-1.35	-2.46	-4.22	-1.28
Std (m/s)	0.59	1.08	0.40	0.37	0.72	0.18

measurements recorded by 3D ultrasonic anemometers, taken in the north-south, east-west and vertical direction (pure quaternion), and the corresponding air temperature (the real dimension of the full quaternion).

Two quaternion models were considered:

- A pure quaternion model where the three orthogonal wind components were used as the vector part of the quaternion signal to form a 3D model;
- A proper quaternion 4D model where the air temperature was added as the scalar part of the model (data fusion via vector spaces [12]- [13]).

Performance was assessed on multistep ahead prediction for the three wind speed components. The first performance index considered was the standard prediction gain R_p, which can be computed as

$$R_p = 10\log_{10}\left(\frac{\sigma_{\mathrm{x}}^2}{\sigma_{\mathrm{e}}^2}\right) \quad [dB] \tag{18}$$

where σ_{x}^2 denotes the variance of the input signal $\{x(n)\}$, and σ_{e}^2 denotes the estimated variance of the prediction error $\{e(n)\}$. For deeper insight, two more performance indices were considered: the error mean B and the coefficient of multiple determination r, given by [25]

$$B = \frac{1}{N}\sum_{n=1}^{N}|x(n) - \hat{x}(n)| \tag{19}$$

$$r^2 = 1 - \frac{\sum_{n=1}^{N}|x(n) - \hat{x}(n)|^2}{\sum_{n=1}^{T}|x(n) - \bar{x}|^2} \tag{20}$$

where N is the number of samples to be predicted, $x(n)$ the actual signal value, $\hat{x}(n)$ is the predicted value, and $\bar{x}$ the mean of the data. The error mean B indicates the bias associated with the error power, whereas r^2 provides a more insightful assessment of the predictor, based on

$$r^2 = \begin{cases} 0 > r^2 & \text{if } \hat{x}(n) \text{ is a worse forecast than } \bar{x} \\ 0 & \text{if } \hat{x}(n) = \bar{x} \\ 0 < r^2 < 1 & \text{if } \hat{x}(n) \text{ is a better forecast than } \bar{x} \\ 1 & \text{if } \hat{x}(n) = x(n) \quad \forall_n \end{cases} \tag{21}$$

A. Simulations on wind data recorded in a controlled environment

This set of simulations was performed on wind data recorded at a sampling frequency of 32 Hz in a controlled environment at ICL. The performance indices, shown in Table II confirm that the additional information from air temperature within the 4D model results in improved accuracies. Although the dynamics of air temperature is quite different from the joint nonlinear dynamics of three orthogonal wind speeds, the quaternionic model naturally allows for the fusion of such heterogeneous data.

In all the scenarios, the predictors based on quaternion statistics significantly enhanced the performance, as compared to the conventional real-valued filter in $\mathbb{R}^4$ both in terms of the bias, coefficient of multiple determination, and the prediction gain.

TABLE II

PERFORMANCE COMPARISON OF THE PREDICTION ALGORITHMS IN $\mathbb{R}^4$ AND $\mathbb{H}$ FOR THE 3D AND 4D WIND MODEL IN A ONE STEP AHEAD PREDICTION SETTING.

	3D Model		4D Model	
Algorithms	MLMS	QLMS	MLMS	QLMS
B	0.016	0.0126	0.013	0.011
r^2	0.697	0.813	0.803	0.999
R_p	5.573	7.66	7.452	8.544

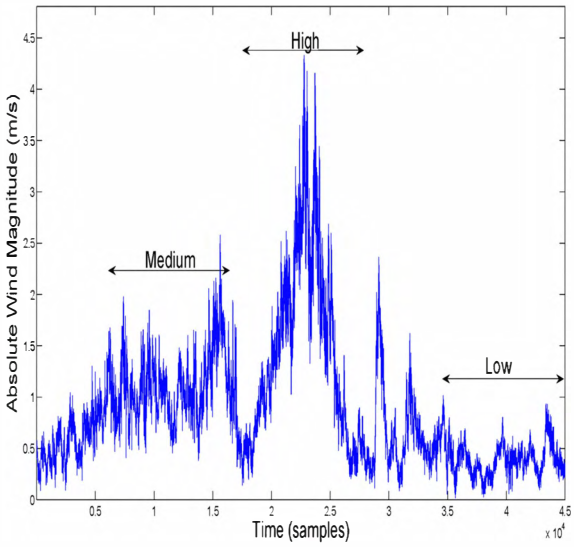

Fig. 3. Magnitude of the 3D wind signal. The wind dynamics regimes are identified as 'low', 'medium', and 'high'.

B. Simulations on wind data recorded in an open space environment

This data set was recorded using a 3D ultrasonic anemometer at a sampling frequency of 50Hz in the courtyard of IIS at the University of Tokyo. To reduce the effects of high frequency noise, the data was preprocessed by a moving average filter, with its window size w_T varying according to

$$w_T = \{1, 2, 10, 20, 60, 300, 600\}$$

Three wind regimes were identified and labelled as 'low', 'medium', and 'high', as shown in Fig. 3. The 3D scatter plot of the wind speeds in the medium wind regime is shown in Fig. 4, and 10,000 samples from each region were taken to train the adaptive predictors. In the first experiment, we investigated the relationship between the prediction gain R_p and the prediction horizon. Fig. 5 shows that the prediction task became more challenging with an increase in the prediction horizon. It is also evident that the QLMS algorithm in $\mathbb{H}$ provided better predictions compared to the MLMS algorithm in $\mathbb{R}^4$. The best prediction performance was obtained for the region with high dynamics; this confirms the benefits of using quaternion statistics, as it

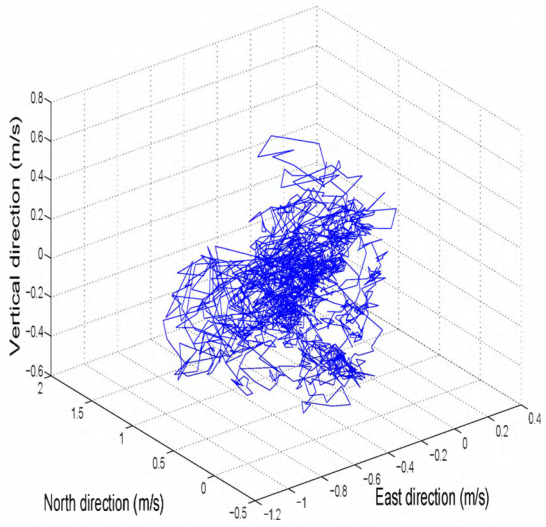

Fig. 4. The 3D scatter plot of wind field (medium regime).

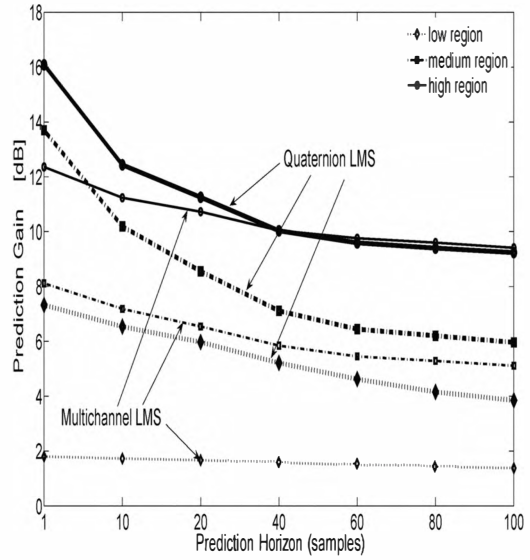

Fig. 5. Prediction gain of QLMS (thick lines) and MLMS (thin lines) algorithms as a function of the prediction horizon for the 3D wind model.

naturally models the coupling between the data components.

Figs. 6 and 7 illustrate the effect of window size of the moving average filter on the prediction gain, that is, the "smoother" the wind data, the better the prediction. Fig. 6 illustrates the simulation results for the 3D model, whereas Fig. 7 shows the improved performances, when the air temperature was considered as the real dimension of the quaternion in the prediction task based on the 4D model. In all the cases, QLMS outperformed MLMS.

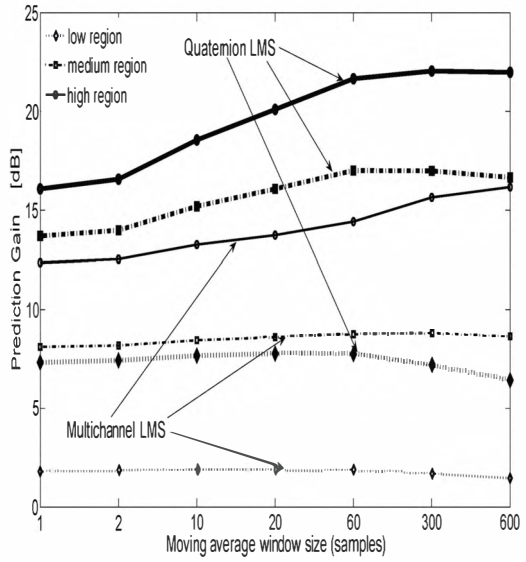

Fig. 6. Prediction gain of the QLMS (thick lines) and MLMS (thin lines) algorithms as a function of the window size of the moving average filter on the 3D wind model.

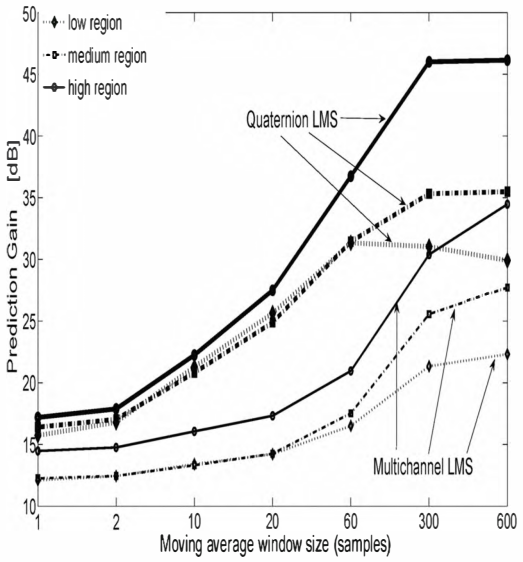

Fig. 7. Prediction gain of QLMS (thick lines) and MLMS (thin lines) algorithms on the 4D wind model, i.e. for the heterogeneous data fusion of the 3D wind field with air temperature.

A snapshot of the estimates of QLMS and MLMS of the four-dimensional quaternion comprising the three components of the wind speed and the air temperature is shown in Fig. 8. The quaternion-valued QLMS algorithm exhibited the ability to track accurately the dynamics of both the wind speeds and the air temperature. On the other hand, the MLMS algorithm could track the air temperature reasonably well, but could only follow the general trend of the highly non-stationary large dynamics of wind speeds. This demonstrates that the QLMS algorithm is a natural choice for the fusion of heterogeneous data, even if the dynamics of data components are radically different, as in the case of the fast changing wind speed and the slow changing air temperature.

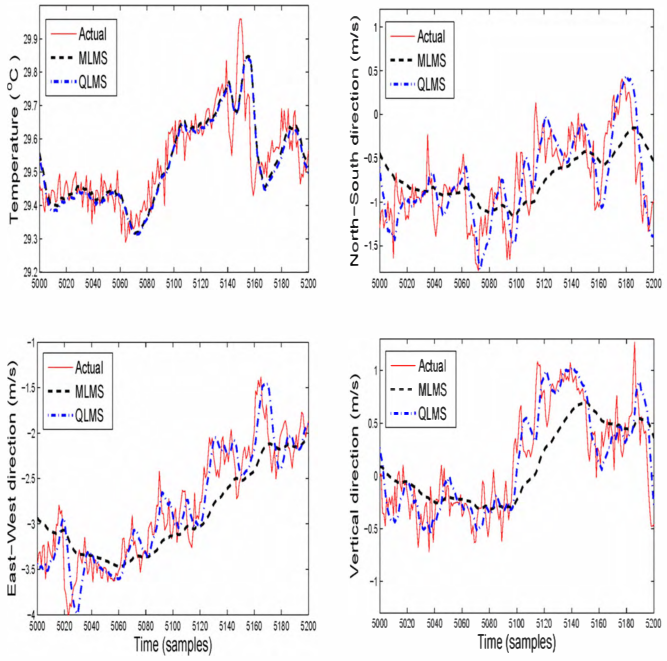

Fig. 8. Predicted estimates of QLMS and MLMS algorithms on the 4D wind field model.

V. Concluding Remarks

This paper has introduced a novel methodology for short term prediction of the wind signal in the quaternion domain. Recent advances in quaternion adaptive filtering have allowed for the fusion of heterogeneous data (3D wind field and air temperature), which led to improved prediction accuracies. It has been shown that the quaternion product naturally takes into account the inter-channel cross-correlation through the outer product. This explains the better performance of the QLMS algorithm compared to the MLMS algorithm, making the former algorithm a preferred choice for short term wind prediction. Simulations on real-world 3D and 4D wind data illustrate the benefits of the proposed direct multidimensional approach.

References

[1] J. C. Smith, Wind Power: Present Realities and Future Possibilities, Proceedings of the IEEE, 97 (2009) 2, pp. 195-197.

[2] E. Hau, Wind Turbines: Fundamentals, Technologies, Application, Economics, Springer (2nd Edition), 2006.

[3] M. S. Roulston, D. T. Kaplan, J. Hardernberg and L. A. Smith, Using Medium-Range Weather Forecasts to Improve the Value of Wind Energy Production, Renewable Energy 28 (2003), pp. 585-602.

[4] M. Ragwitz and Kantz, Detecting Non-Linear Structure and Predicting Turbulent Gusts in Surface Wind Velocities, Europhysics Letters, 51 (2000), p. 595-601.

[5] H. Kantz, D. Holstein, M. Ragwitz and N. K. Vitanov, Markov Chain Model for Turbulent Wind Speed Data, Physica A, 342 (2004), pp. 315-321.

[6] Y. Hirata, D. P. Mandic, H. Suzuki and K. Aihara, Wind direction modelling using multiple observation points, Philosophical Transactions of The Royal Society, 366 (2007), pp. 591-607.

[7] S. L. Goh, M. Chen, D. H. Popovic, K. Aihara, D. Obradovic and D. P. Mandic, Complex-valued forecasting of wind profile, Renewable Energy 31 (2006) 11, pp. 1733-1750.

[8] D. P. Mandic, S. Javidi, S. L. Goh, A. Kuh and K. Aihara, Complex-valued prediction of wind profile using augmented complex statistics, Renewable Energy 34 (2009) 1, pp. 196-201.

[9] M. C. Alexiadis, P. S. Dokopoulos, H. S. Sahsamanoglou and I. M. Manousaridis, Short term forecasting of wind speed and related electrical power, Solar Energy 63 (1998) 1, pp. 61-68.

[10] S. Li, D. C. Wunsch, E. A. O'Hair and M. Giesselmann, Using NNs to estimate wind turbine power generation, IEEE Transaction on Energy Conversion 16 (2001) 3, pp. 276-282.

[11] S. Mathew, Wind Energy: Fundamentals, Resource Analysis, and Economics, Springer, 2006.

[12] D. P. Mandic, S. L. Goh, and K. Aihara, Sequential Data Fusion via Vector Spaces: Fusion of Heterogeneous Data in the Complex Domain, The Journal of VLSI Signal Processing Systems, 48 (2007), pp. 99-108.

[13] D. Mandic, M. Golz, A. Kuh, D. Obradovic, and T. Tanaka (Editors), Signal Processing Techniques for Knowledge Extraction and Information Fusion [Information Technology: Transmission, Processing and Storage], (2008) Springer.

[14] D. Mandic and S. L. Goh, Complex Valued Nonlinear Adaptive Filters: Noncircularity, Widely Linear and Neural Models, (2009) Wiley.

[15] C. Cheong Took and D. P. Mandic, The Quaternion LMS Algorithm for Adaptive Filtering of Hypercomplex Real World Processes, IEEE Transactions on Signal Processing 57 (2009) 4, pp. 1316-1327.

[16] C. Cheong Took, D. P. Mandic, and J. Benesty, Study of the Quaternion LMS and Four-channel LMS Algorithms, International Conference on Acoustics, Speech and Signal Processing, Taiwan (2009), pp. 3109-3112.

[17] Y. Huang and J. Benesty, Audio Signal Processing for Next Generation Multimedia Communication Systems, Kluwer Academic Publishers, 2004, pp. 132-133.

[18] E. Wan, Time series prediction using a neural network with embedded tapped delay-lines. In: Predicting the future and understanding the past, SFI studies in the science of complexity (1993), pp. 195-217.

[19] H. Toyoshima, Computationally efficient implementation of hypercomplex digital filters, IEEE International Conference on Acoustics, Speech and Signal Processing (1998), pp. 1761-1764.

[20] Y. Furman, R. Khafizov and A. Rozhentsov, Filtering of quaternion signals, Journal of Communications Technology and Electronics 52 (2007) 1, pp. 36-44, 2007.

[21] T. Bülow and G. Sommer, Hypercomplex signals - a novel extension of the analytic signal to the multidimensional case, IEEE Transactions on Signal Processing 49 (2001) 11, pp. 2844-2852.

[22] S. Said, N. L. Bihan and S. J. Sangwine, Fast complexified quaternion Fourier transform, IEEE Transactions on Signal Processing 56 (2008) 4, pp. 1522-1531.

[23] N. L. Bihan and J. Mars, Singular Value Decomposition of Quaternion Matrices: A New Tool for Vector-Sensor Signal Processing, Signal Processing 84 (2004) 7, pp. 1177-1199.

[24] S. Haykin and L. Li, Nonlinear adaptive prediction of nonstationary signals, IEEE Transactions on Signal Processing 43 (1995) 2, pp. 526-535.

[25] R. Drossu and Z. Obradovic, Rapid design of neural networks for time series prediction, IEEE Computational Science and Engineering 3 (1996) 2, pp.78-89.